Finite Element Analysis Validation in Ball Bearing and Linkage Assemblies for Exoskeleton Robotics

A Thesis
Presented in Partial Fulfillment of the Requirements for the
Degree of Master of Science
with a
Major in Mechanical Engineering
in the
College of Graduate Studies
University of Idaho
by

Anthony J. Branz

Major Professor: Joel Perry, Ph.D.
Committee Members: Daniel Robertson, Ph.D.; Eric Wolbrecht, Ph.D., P.E.
Department Administrator: Steven Beyerlein Ph.D.

December 2019

AUTHORIZATION TO SUBMIT THESIS

This thesis of Anthony J. Branz, submitted for the degree of Master of Science with a Major in Mechanical Engineering and titled "Finite Element Analysis Validation in Ball Bearing and Linkage Assemblies for Exoskeleton Robotics," has been reviewed in final form. Permission, as indicated by the signatures and dates below, is now granted to submit final copies to the College of Graduate Studies for approval.

Major Professor:	_____	Date:	_____
	Joel Perry, Ph.D.		
Committee Members:	_____	Date:	_____
	Eric Wolbrecht, Ph.D., P.E.		
	_____	Date:	_____
	Daniel Robertson, Ph.D		
Department Administrator:	_____	Date:	_____
	Steven Beyerlein, Ph.D.		

Abstract

Stroke is one of the leading causes of disability in the world today. Many individuals who have suffered a stroke experience upper-extremity impairment, reducing their quality of life. Studies have suggested that with proper rehabilitation and assessment these individuals can achieve greater recovery, thus improving the lives of many. BLUE SABINO, an exoskeleton being developed at the University of Idaho, is being designed to help assess these stroke patients as well as assist in the rehabilitation process. One of the greatest challenges while designing an exoskeleton is keeping it lightweight while simultaneously ensuring adequate rigidity. Finite element analysis (FEA) is an engineering tool that allows computer models, of structural assemblies/components, to be simulated under specified loading conditions. For structural applications these simulations result in estimates of stresses, strains, and deflections. This tool allows engineers to assess a variety of scenarios rapidly without manufacturing physical components, saving money and time during the design process. However, careful implementation is required to achieve accurate results. This thesis describes three experiments that are compared to their FEA counterparts to check the validity of the solution. One of the assemblies acted as a control test, only featuring bolt connections. The other two assemblies consisted of similar bolt connections while also including multiple bearing connections. The control test was used to find an optimal mesh that kept simulation times low without compromising accuracy and resulted. Comparing the simulation to the experimental data resulted in an error 6.6%. While performing the simulations for the bearing tests, axial and lateral stiffness values could be assigned to the bearings. An optimal value of 3.5e7 N/m (lateral stiffness) and 3.75e5 N/m (axial stiffness) was determined, resulting in solutions with errors of -1.04% and -0.28% at a load of 200N. Using these optimized stiffness values while varying the simulation's applied load resulted in increased error for both models, with a maximum error of 24.6%. These results show that FEA can be used to accurately predict deflections in bolted and bearing connections used in exoskeletons and provided insight that the bearings were the main source of deflection within the assembly.

Acknowledgment

First off, I would like to thank Dr. Joel Perry. Without your support none of this would have been possible. Your assistance goes back to when I was on your team for senior Capstone and has always been appreciated. I couldn't have asked for someone better to have around for brainstorming, guidance, or just to chat with. Your work ethic is something that was truly inspiring and helped drive me to work far harder than ever to achieve my goals. I am also grateful that I was able to be a teacher's assistant for your SolidWorks classes over the semesters. It was incredibly helpful to be able to work at the school, while simultaneously funding my Masters. Most of all I am thankful for your support editing and guiding me through this thesis as it was a true challenge for me and something I can now be proud of.

I would also like to thank Dr. Eric Wolbrecht. Our acquaintance began my freshman year when you became my advisor. Your guidance is one of the main reasons I decided enroll in the Masters program and I cannot thank you enough as I now feel ready to tackle any problem ahead of me. You lead me through college as well as taught me many topics over the years with exceptional skill. I would also like to thank you for allowing me to be a teacher's assistant for your lab. This gave me a better understanding of how to perform laboratory experiments and how to teach (which is harder than I first anticipated).

I would also like to thank all of my committee members Dr. Joel Perry, Dr. Eric Wolbrecht, and Dr. Daniel Robertson. Thank you for taking the time to assist in editing my thesis, attending my defense, and helping me complete the experiments discussed in this paper.

Finally I would like to thank the team I work with over my two years on the project: Chris Bitikopher, Rene Maura, Melissa Bogert, Parker Hill, and Sabastian Rueda. I enjoyed every minute working with you all and couldn't have asked for a better team. Beyond this, I feel like I have made some great friends in all of you and hope our paths cross once again.

Dedication

I dedicate my work to my family.

First and foremost to my parents, Anthony and Jennifer Branz, who over the last quarter-century have supported and drove me to become the man I am today. You two have very busy lives, but always found time for all of your children. In this time you gave us the tools we needed to succeed and when the time came, a pat on the back for our accomplishments. You two were always there whether it was a sporting event or a graduation and I am so thankful. Dad, you taught me that you can achieve anything if you put your heart into it and gave me a drive that I would not have had without you. Mom, I would make a sly joke here for you, but I know you would come back with a better one, and since this is getting published, I don't want to bring that evil upon myself. You two did everything for us so thank you both, I love you.

To my three younger siblings: Curtis, we are literally polar opposites, but I'm glad we are becoming closer now that we are both growing up. Believe it or not, you taught me so much and, without you, I'm sure I would have gotten in a lot more trouble as a kid. Dom, you showed me the art of taking the path of least resistance. I am still baffled on how you were able to tread so carefully that you could almost get away with murder growing up. Katy, I know it had to have been a bit rough being the youngest and the only girl, but you crushed it. I love you all, and cannot wait to see what the future has in store for us.

Table of Contents

Authorization to Submit Thesis ii
Abstract iii
Acknowledgment iv
Dedication ii
Table of Contents iii
List of Figures v

1 Introduction 1
1.1 Motivation 1
1.2 Background: BLUE SABINO 2
1.3 Background: Bearing Models 4
1.4 Background: Finite Element Analysis 5
1.5 Overview 6

2 Finite Element Analysis 8
2.1 General Steps of Structural Finite Element Analysis 8
2.2 Part Configuration/Creation 10
2.3 Meshing 13
2.4 Fixtures 15
2.4.1 Fixed 15
2.4.2 Roller/Slider 17
2.4.3 Fixed Hinge and Bearing 18
2.5 Connectors 19
2.5.1 Pin Connectors 19
2.5.2 Bolt Connectors 20
2.5.3 Bearing Connectors 21
2.6 Contacts 22
2.7 Forces 24

3 Methods 27
3.1 Overview 27

3.2 Control Test....28
3.3 Bearing Tests....29
3.4 FEA: Control Test....30
3.5 FEA: Upper and Lower Bearing Test....31

4 Results....34
4.1 Control Test....34
4.2 FEA: Determining Bearing Stiffness....36
4.3 FEA: Variable Force Bearing Test....38
4.4 Control Test Discussion....40
4.5 Bearing Tests Discussion....40

5 Concluding remarks....42
5.1 Previous FEA Methods....42
5.2 Future Work....42
5.3 Closing Remarks....43
References....44

List of Figures

Figure 1-1: A rendering of the right arm of BLUE SABINO and 1005 assembly 3
Figure 1-2: Example results from SolidWorks FEA..... 6
Figure 2-1: An example of the use of the split-line tool 10
Figure 2-2: An example of how geometric imperfections can cause significant differences in FEA results..... 12
Figure 2-3: An example mesh applied to a 2-dimensional shape for the purpose of FEA. 14
Figure 2-4: An FEA simulation using fixed fixtures, represented by green arrows, to illustrate a correct use of this option 16
Figure 2-5: An example of a *roller/slider* fixture being applied to a face within SolidWorks simulation..... 17
Figure 2-6: An example of the implementation of a displacement boundary condition 18
Figure 2-7: Illustration of how a *fixed hinge* restraint functions within SolidWorks. 18
Figure 2-8: Illustration of how bearings are modeled within SolidWorks. (Dassault Systemes, 2019) 22
Figure 2-9: Bonded contact set. Image from (King, 2018). 23
Figure 2-10: No-penetration contact with load causing gap. Image from (King, 2018) 24
Figure 2-11: Allow-penetration contact being used under two loading conditions. Image from (King, 2018)..... 24
Figure 2-12: Example of Saint Venant's principle. Image from (Sonnerlind, 2018). 26
Figure 3-1: Assembly 1005 of the Blue Sabino project..... 28
Figure 3-2: Control test to verify FEA without bearings. 29
Figure 3-3: Experimental bearing test setups with the left being the *lower bearing* test and the right being the *upper bearing* test. 30
Figure 3-4: Control Test FEA setup..... 31
Figure 3-5: FEA setup for *upper* and *lower* bearing test.. 33
Figure 4-1: Results of the seven experimental control tests 34
Figure 4-2: Results for control test with varying meshes 35

Figure 4-3: Raw simulation data generated by varying the axial and lateral stiffness values in the bearing test. 37
Figure 4-4: Graphical representation of how changing the axial and lateral stiffness affects the cost function. 38
Figure 4-5: Comparison of the experimental and simulation results over a range of 250N for the *upper* bearing test and 150N for the *lower* bearing test 39

1 INTRODUCTION

1.1 Motivation

Every 40 seconds someone in the United States (US) suffers a stroke, resulting in more than 795,000 strokes per year in the US alone (Mozaffarian Dariush et al., 2016). After having a stroke the likelihood of disability increases more markedly than any other condition (Adamson et al., 2004). In 2000, the age-standardized stroke death rates were 118.4 per 100,000 persons among adults older than 34. By 2015, this rate declined 38% to 73.3 per 100,000 persons. This decline is attributed to improvements in modifiable stroke risk factors, stroke treatment, and care over time (Lackland et al., 2014). These factors make stroke one of the leading causes of serious long-term disability among adults.

Strokes occur in one of two forms: ischemic or hemorrhagic. Ischemic strokes account for roughly 87% of all strokes within the US (Benjamin et al., 2017). An ischemic stroke occurs when an artery to a localized region of the brain is blocked, cutting off blood flow and resulting in oxygen loss to the brain cells in the affected region. If oxygen is lost for an extended period of time these brain cells begin to die and their contribution toward functions such as memory, muscle control, and speech are lost. However, some motor function will naturally recover over time, and by increasing the intensity of post-stroke therapy, greater recovery results can be achieved. This recovery is a result of the brain remapping the lost functions to other locations within the brain (Schaechter, 2004). The most significant recovery has most commonly been documented between 2 weeks and 3 months after a stroke followed by a plateau in improvement (Skilbeck et al., 1983), (Kelly-Hayes et al., 1989). However, other studies have shown that, with novel rehabilitation regimens, patients that have “plateaued” with standard clinical scales can further improve motor functions (Page et al., 2004).

The number of strokes double each decade after the age of 45 with over 70% of all strokes occurring above the age of 65 (Kelly-Hayes, 2010). It is projected that by 2030 all of the “baby boomers” will be above the age of 65 (Bureau, 2019). Additionally, of all the individuals who have survived a stroke, nearly half have moderate to severe neurological

damage with some being unable to walk and over 25% needing assistance with tasks of daily living (Kelly-Hayes, 2010). This projection, along with lower mortality rates, predicts a tremendous strain on the healthcare system for decades to come. Without proper care, the number of individuals suffering from long-term disability will increase. Due to this reality, the development of novel systems that ensure individuals receive proper care and the means to live unassisted after a stroke are needed. One promising solution is the use of robotic devices that assist in the assessment and rehabilitation processes following a stroke. Such devices will reduce the load on caregivers through the automation of post-stroke rehabilitation while also providing increased assessment accuracy, ultimately improving overall care following a stroke.

1.2 Background: BLUE SABINO

The University of Idaho's BLUE SABINO (Bi-Lateral Upper-extremity Exoskeleton for Simultaneous Assessment of Biomechanical and Neuromuscular Output) is one example of an exoskeleton that will improve upon current post-stroke metrics through advanced assessment tools as well as aid in the rehabilitation process. BLUE SABINO is a 30-degree-of-freedom (DOF) dual arm exoskeleton with high-torque actuation, precision force/torque sensing, electroencephalography (EEG) sensors, and electromyography (EMG) sensors. The 30 DOFs allow for assistance in natural reaching and grasping tasks common in many activities of daily living, while the force/torque sensing allows for the monitoring of forces being generated by the patient. The exoskeleton's sensors and kinematics allow for the patient's range of motion to be recorded. The EEG and EMG sensors are used to monitor the neuromuscular pathways patients use following a stroke to further the understanding of impairment and the recovery process. All of these sensors will function simultaneously and will record in real-time allowing for rapid assessment along with a quantitative description of the patients' impairment. The data provided during an assessment should improve metrics, allowing for more specialized, targeted therapies that can improve patients' overall recovery.

BLUE SABINO, Figure 1-1, is an extension of the EXO-UL series exoskeletons developed by Rosen et al. (Perry and Rosen, 2006). More specifically, the EXO-UL7 (Simkins et al., 2013) and the EXO-UL8, which moved away from the cable-driven design by

implementing Harmonic Drive motors at the joints for actuation (Shen et al., 2018). BLUE SABINO improves upon the design of the EXO-UL8 by adding two additional DOFs at the shoulder that allow for vertical and horizontal translation of the shoulder joint. BLUE SABINO also incorporates remote center, parallel-linkage mechanisms that allow for easier donning and doffing of the device while retaining the ability for axial rotation of the arm segments. This mechanism is complicated, consisting of 14 bearing connections, making the determination of deflection difficult. Due to its complexity and the importance of rigidity in exoskeleton structures, this mechanism will be a focus of this paper.

Figure 1-1: A rendering of the right arm of BLUE SABINO and 1005 assembly. The left images illustrates the exoskeleton interacting with a mannequin and the right shows the remote center, parallel-linkage mechanism used for internal/external rotation of the arm.

One major design challenge in any exoskeleton, especially devices with active joints, is the minimization of weight and deflection. Excessive deflection leads to vibration problems, a lower natural frequency, and inaccurate position measurements. However, minimizing weight and deflection simultaneously is challenging, as additional supporting material typically reduces deflection while increasing weight. Other unnecessary material increases the overall weight, while not improving the strength in the primary modes expected during operation. Furthermore, any excess mass in the distal links of the exoskeleton require stronger,

likely heavier, components upstream which can in turn require larger motors. Due to the nature of this problem, the components of BLUE SABINO should be as lightweight as possible without compromising the overall stiffness of the device. To accomplish this, finite element analysis (FEA) has been extensively used throughout the design process to optimize components and assemblies, resulting in components with high stiffness and minimal mass.

1.3 Background: Bearing Models

Studies on rolling element bearings date back to 1946 with Jones investigating the nonlinear relationship between deflection and applied load (Jones, 1946). Palmgren (Palmgren, 1959), Harris (Harris, 1990), and Brandlein (Brandlein et al., 1999) followed, with Gargiulo establishing empirical formulae that related the load-stiffness and deflection-stiffness (Gargiulo, 1980). However, these formulae, along with the other theoretical studies, are limited to a few types of bearings. Also these studies cannot determine tilting and cross-coupling stiffnesses between the radial, axial, and tilting deflections of bearings (Guo, 2012). Further theoretical models were proposed to estimate diagonal and cross-coupling terms in the stiffness matrix (Lim, 1990), estimate the stiffness matrix by dividing the rolling element surface (Bourdon et al., 1999), and include time-varying stiffness caused by orbital motion of the rolling elements (Liew etal., 2005).

These models all make different critical assumptions about the contact between the rolling elements and races. These differences result in great discrepancy when estimating bearing stiffnesses. Discrepancies also exist due to bearing details not being included in the model that affect bearing stiffness, such as: internal radial and axial clearances, roller and race crowning, race width and thickness, diameter of the inner raceway, and bore of the outer raceway. Due to the absence of critical information stiffness estimates provide limited accuracy with many limitations (Guo, 2012).

Newer studies, performed by Guo, use finite element methods to determine the stiffness matrix associated with rolling bearings. This study captured the coupling between radial, axial, and tilting deflections of the bearings. The solution was validated against experiments, but

without knowing the exact solutions in common use, an iteration scheme was implemented to help estimate the accuracy of the results (Guo, 2012).

Solidworks uses a simpler model that treats bearings as spring elements and will be discussed in further detail in section 2.5.3.

1.4 Background: Finite Element Analysis

Finite element analysis comes from the finite element method (FEM) which is a way to combine computational power, numerical methods and physics to solve complicated engineering problems that may otherwise prove too difficult (Logan, 2016). FEMs have the ability to solve problems in thermal/fluid flow, mass transport, electromagnetics, soil mechanics, acoustics, structural mechanics and more. This makes it a valuable tool in a wide range of applications including but not limited to aeronautical and automotive design, implant analysis, meteorological fluid flow problems, and robotics. The application of FEMs within a specific field are often referred to as a FEA.

FEMs have become one of the most useful analysis tools for engineers in the modern age due to their versatility among a wide variety of applications fields and their ability to solve complex problems. There are several advantages to FEA including flexibility, cost savings, and ability for rapid visualization showing how systems react under given conditions. Since deflection and mass minimization are major design challenges for the BLUE SABINO project, FEA can be used to influence the design process. Structural analysis, within SolidWorks Simulation, will be used to optimize components, and will be the primary field of FEM discussed in this paper.

FEA results are commonly displayed as colored heat maps or graphs that illustrate stresses and deflections throughout a component or assembly. Their results are derived from post-processing steps that determine the integrals or derivatives at nodes, discussed in section 2.4. An example of an FEA result can be seen in Figure 1-2. Other post-processing steps can yield error estimates that can help optimize the study in poorly preforming regions.

1.5 Overview

FEA is a complicated process that without careful implementation can result in invalid results and poor design decisions. To minimize the occurrence of such mistakes, the following chapters describe the general use of FEA, the methods/results of an FEA verification experiment, and a discussion of the validity of a simulation compared to the physical experiment.

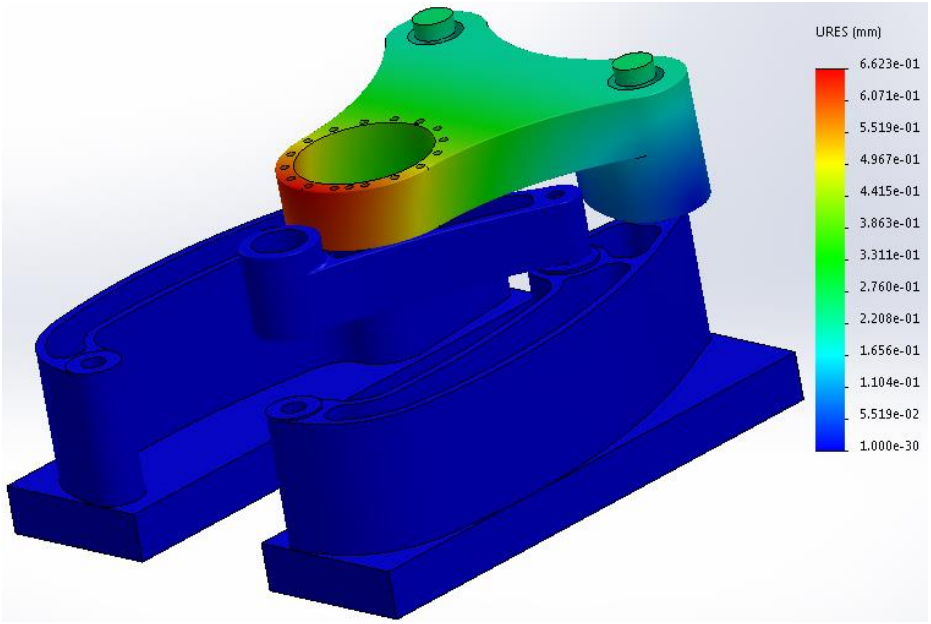

Figure 1-2: Example results from SolidWorks FEA. The image shows the results from a displacement test on an assembly within the BLUE SABINO project. The color bar on the right illustrates the magnitude of deflections throughout the assembly, red being the highest with a value of 0.66mm.

Chapter 2 discusses the general steps that take place during the FEA process along with best practices for configuring parts, implementing fixtures, and applying forces. Also discussed are several features available within SolidWorks to further the understanding of tools available while performing FEA. These features include a variety of fixtures, connectors, and contact sets that if used improperly can result in inaccurate solutions. Chapter 3 describes the methods used to perform an experiment that compares the deflection of an assembly within BLUE SABINO to the same assembly modeled within FEA. This assembly has multiple bearing connections that, if not modeled correctly, lead to significant errors within the simulation.

Chapter 4 presents the FEA and experimental results along with a discussion of the validity of the simulation. Finally, Chapter 5 provides closing thoughts and remarks as well as a discussion on previous FEA methods used within the BLUE SABINO project that ultimately lead to the method discussed in this paper.

2 FINITE ELEMENT ANALYSIS

2.1 General Steps of Structural Finite Element Analysis

FEA is a multistep process that systematically solves complex problems. The steps are as follows:

1. Discretization of the domain (Meshing)
2. Establishing primary and secondary unknowns
3. Establishing displacement function
4. Establishing stiffness matrix
5. Derivation of global equation
6. Solving for primary and secondary unknowns

The process of discretizing the domain, (*i.e. meshing*), refers to the division of the load-bearing body into finite elements that are used to solve an overall problem. Meshing allows a large problem to be solved as many smaller problems, resulting in the ability to solve problems with high levels of complexity. Meshing will be discussed further in section 2.4, but from this process, elements and nodes are formed.

For structural FEA, the primary unknowns are the nodal displacements with strain and stress being secondary unknowns. This is because the secondary unknowns can easily be solved using the nodal positions and the nodal displacements found using displacement functions. Displacement equations are assigned to each element and are defined using the neighboring nodes. These functions are typically linear, quadratic, or cubic polynomials as these are easiest to use within finite element formation (Logan, 2016).

For a structural application the stiffness matrix defines the relationship between strain/displacement and stress/strain. Considering a one-dimensional problem, the strain/displacement relationship is:

$$\varepsilon_x = \frac{du}{dx} \tag{2-1}$$

where ε_x is the strain in the x direction and is related to the displacement u (Logan, 2016). Constitutive laws are implemented to relate the strain/displacement relationship to the material properties of the specimen being tested. One example of a constitutive law is Hooke's law, given as:

$$\sigma = E\varepsilon \tag{2-2}$$

where σ is the stress, ε is the strain, and E is the modulus of elasticity. There are other methods to derive the stiffness matrix such as the direct equilibrium method, work or energy method, and weighted residual method, but for each case, the stiffness equations are applied to the nodes on each finite element.

Individual element nodal equations and the stiffness equations are assembled into a global equation. During this step, boundary conditions, such as fixtures and external forces, are implemented. This process is completed through the method of superposition, also referred to as the direct stiffness method. The direct stiffness method solves for all nodal forces in equilibrium, resulting in an equation with displacements as the only unknowns. This method also applies the concept of continuity, which means that the body cannot tear apart, but will instead continue to stretch indefinitely (Logan, 2016).

The primary unknowns are solved using an elimination method, such as Gaussian elimination. From this process, the displacements are calculated at each node. The secondary unknowns can then be solved using these known displacements. There are several methods of interpreting the results. SolidWorks uses color maps and components in their deformed state to illustrate how a model reacts to given forces and restraints, as seen above in Figure 1-2.

2.2 Part Configuration/Creation

When configuring an assembly for FEA simulation, several considerations should be taken into account to ensure proper meshing, restraining, and connections along with ensuring the overall accuracy of the model. Small geometric and assembly flaws can have large effects on the results as they can cause falsely high stresses or incorrect deformations. The restraints and loading conditions also need to be considered, and often require application to sub-areas of modeled faces rather than across an entire face. SolidWorks' split-line tools will most likely be needed in order to create selectable sub-faces to accurately represent how a component will interact with its surroundings. Split-lines are features within SolidWorks that allow specific selectable faces to be created without geometric modifications. Split-lines are often necessary because the faces required for implementing forces or using connectors are typically not created during the modeling phase. Figure 2-1 illustrates how split-lines can be applied. The left image illustrates the selectable surface without split-lines while the right shows a refined selection by the use of split-lines. With the split-lines shown in the right image forces can be applied to the small selected religion rather than the entire face, allowing for more customization during the FEA process.

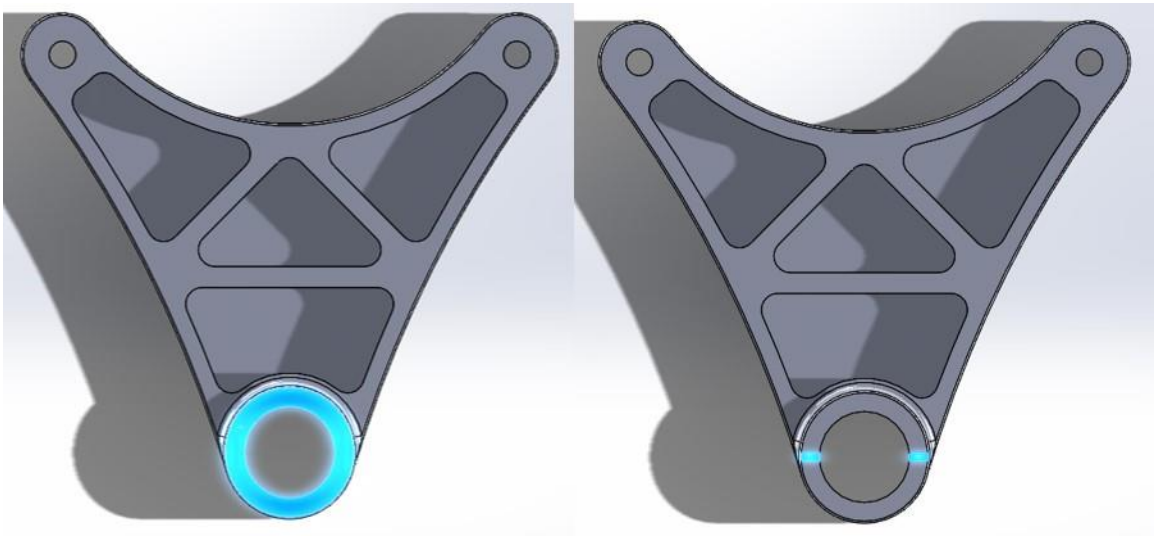

Figure 2-1: An example of the use of the split-line tool. The left image is without split-lines, causing the entire surface to be selected. The right images has split-lines, allowing for specific regions of the surface to be selected.

Drafted components and assemblies that are intended for FEA simulation need to be correctly modeled as small errors in modeling can result in significant errors in FEA results. While a component may appear to be perfect at a glance, a closer look could disclose small errors such as tiny surface imperfections, internal voids, or odd fillets. These small errors can result in mesh failures or high stress concentrations. An exaggerated example of how a small imperfection can affect a simulation is illustrated in Figure 2-2. From the top two images, the component appears to be correct. However, there is a small crease along the base of the cylinder, and without closer inspection the user is unable to see this imperfection. Small imperfections such as this crease can be created by accidentally selecting wrong profiles during modeling, or making sub-optimal end-condition selections during 3D feature creation. For example, using a “blind” extrude rather than “up to surface” when a feature should always extrude fully into another existing surface in the model. The risk of errors becomes more likely if components are not carefully modelled, taking into account potential modifications that may be needed during the design process. The bottom-right image shows FEA results of the incorrect part and the bottom-left show the results of the part modelled correctly. For both cases the exact same FEA parameters were used, including the deformation scale. This example shows that slight errors in the geometry can cause large differences in the results. In less exaggerated scenarios the imperfection could easily be overlooked.

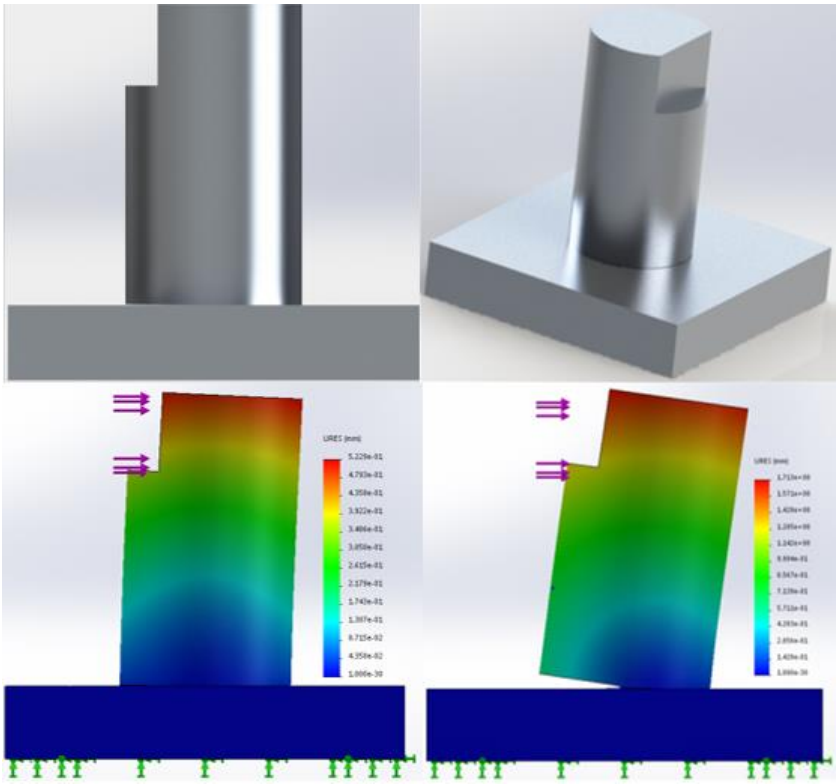

Figure 2-2: An example of how geometric imperfections can cause significant differences in FEA results. The top two images show the same part that has a small crease at the base of the cylinder that is very difficult to see without zooming in. The bottom-left shows FEA results if the imperfection is corrected while the bottom-right shows the results if the imperfection was overlooked.

When preparing a simulation some features can be removed, such as raised logos that are not entirely required for the component's functionality. Removing such features can save computation cost, but as seen above, small changes can have large impacts on the results. This means the user must decide if removing a feature will adversely affect the study. For example, consider the removal of a small fillet. If a small fillet is removed, the number of elements required in the mesh is reduced, but it may create a sharp reentrant corner that can yield stresses that are high and incorrect (Akin, 2010). This overly high, false stress could easily cause the user to miss a critical, high-stress location that can lead to component failure. This user oversight occurs due to the heat map, used to illustrate the magnitudes of stresses and deflections, being automatically scaled to the largest value present, following each simulation.

When high stresses exist, critical locations may become overshadowed as the stresses at these locations are colored to more closely resemble the less severe portion of the heat map.

Along with the importance of the component's geometrical accuracy, the assembly must be configured correctly. This means it is imperative there are no interferences and that coincident components are correct. In SolidWorks, this can be done with the Interference Detection tool. This tool allows the user to see interferences, along with the ability to see every touching face within the assembly. This should be done before any assembly simulation setup, as incorrect interferences or contact points could result in reconfiguring the entire FEA setup.

Finally, the method in which the component will be restrained in space must be considered. This is done by applying fixtures, discussed in section 2.5, and should be done in the manner that most accurately represents how the component is restrained in its real-world application. Fixtures can be used directly on the component as long as they do not compromise the study. Otherwise, drafting mock components or using more of the surrounding assembly can be effective. Using mock components or adding more of the assembly moves the fixture farther away from the critical component and can improve the simulation's results.

2.3 Meshing

Meshing refers to the process of the division of a body or shape into a number of smaller, simpler shapes called finite elements. These elements are typically configured as triangles, quadrilaterals, tetrahedrals, or hexahedrals. Figure 2-3 shows an example of a 2-dimensional mesh generated using SolidWorks. This image illustrates how many simple finite elements can be combined to sum to a larger, more complicated shape. SolidWorks uses quadratic tetrahedral element in its meshed components. Generally, hexahedral elements are more accurate, but by using more tetrahedral elements, the results are comparable and creating the mesh automatically becomes more reliable (Akin, 2010). The mesh nodes discussed previously are located at the intersection of the elements, and these junctions are the points where calculations are performed.

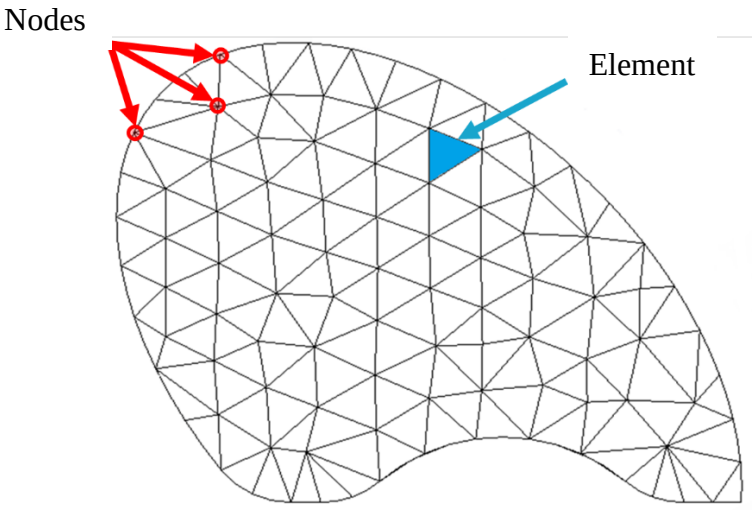

Figure 2-3: An example mesh applied to a 2-dimensional shape for the purpose of FEA.

SolidWorks FEA allows the user to define the maximum and minimum element size as well as adjust the growth rate from element to element. Beyond this, three types of meshes can be applied: *standard mesh*, *curvature-based mesh*, and *blended curvature-based mesh*. Using these settings to increase element number or change the shape increases computational cost, but reduces error. The mesh should be refined around common engineering curves such as circular arcs, splines, and nubs as the mesh fits with a polynomial and will have geometric errors if the mesh is too coarse. It is also important to refine meshes in regions where high stress gradients are expected (Akin, 2010). Common locations for these high stress gradients are at the loading and support regions. However, refining the mesh can significantly increase computational cost, ultimately leading to longer simulation times or potentially exceeding available hardware's capabilities. To reduce computational cost, coarse meshes can be used in regions with easy-to-fit shapes and regions with low stress gradients. This can slightly reduce accuracy, but if coarse mesh regions are carefully selected, the error is negligible and simulation times are dramatically reduced. Within SolidWorks, mesh controls can be implemented to designate specific mesh sizes in various locations. Ultimately it is up to the engineer's judgement to decide where the mesh needs to be changed.

Lastly, while using SolidWorks FEA, it is recommended to attempt to mesh the study before applying contacts, fixtures, and forces, as those steps can be time consuming and may have to be repeated if the mesh fails.

2.4 Fixtures

Fixtures are the supports that restrain a model and are one of the most common sources of error while setting up an FEA. Engineers have used simplified concepts to restrain structural problems for decades. Common simplified supports include fixed, roller, and pin connections. These simplified concepts define the three translational degrees of freedom (DOFs), along with the three rotational DOF in a system and within FEA are referred to as the "Dirichlet boundary conditions" (Akin, 2010). These simplified concepts are the fixtures used within most mechanical FEA approaches, including SolidWorks. Since these are simplified models, it becomes easy to choose fixtures that do not accurately represent how components interact with their supporting material.

When restraining a model with fixtures, it is important to find the method that most closely represents how the component interacts with its surroundings. As stated above, including mock components or more of the surrounding material can help improve simulation results. This is a result of the force being located farther away from the fixture. If the fixture is too close to the applied force, incorrect, high-stress regions can form as the specific fixtures can restrict all motion. These surrounding components can also be made rigid if the focus of the study is only on one component, but this option can often translate the fixtures properties to the critical component and should be carefully considered before implementing.

In the following subsections, the function of *fixed*, *roller/slider*, *bearing*, and *fixed hinge* fixtures will be discussed, along with best practices to avoid errors during implementation.

2.4.1 Fixed

When choosing the *fixed* fixture option, the selected entities are restrained in all directions, thus not allowing deformation or movement in any of the six DOFs. Since complete

restriction of a face is usually an unrealistic constraint, large errors can form within an FEA if not used carefully. These errors mainly appear when looking at stresses, but can also affect the overall displacement of the model. This is because incorrect fixed surfaces can result in overly high stresses on the fixed face. *Fixed* fixtures should be placed in low stress regions with sufficient distance from the external load to help ensure they do not compromise the study. The *fixed* fixture being used can be seen in Figure 2-4. The green arrows on the base of the assembly represent the fixed faces, while the purples arrows represent an external force. In this assembly's application the two base plates are fastened to a sturdy table resulting in negligible deflection/stress on the bottom of these plates, meaning the *fixed* option is appropriate.

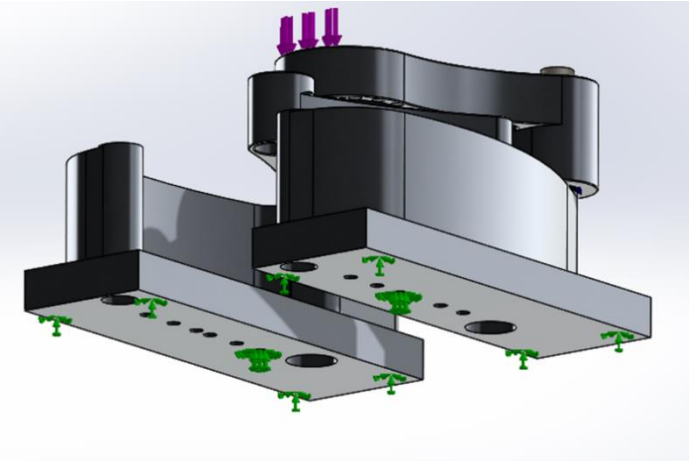

Figure 2-4: An FEA simulation using fixed fixtures, represented by green arrows, to illustrate a correct use of this option. This application of the fixed fixture is appropriate because the fixtures are located in low-stress regions and distant from the external load. These fixtures also closely match the real-world application, as the restrained face was bolted on a table.

In SolidWorks, lines can also be selected while using the fixed restraint. By fixing an edge or line rather than a surface, SolidWorks will model that location as a "fixed-pinned" connection. Meaning the component will not be allowed to translate, but rotation will be free about the axis of the selected line/edge. This can be useful while modeling hinge points within a model as the *fixed-pinned fixture* is only for cylindrical faces.

2.4.2 Roller/Slider

While using the *roller/slider* fixture, a planar face is selected and is free to move parallel to the plane, but cannot move in the direction normal to the plane. With this restraint, the face can also shrink or expand depending on the loading conditions. When using this restraint other fixtures will be required in order to perform a static simulation, as one *roller/slider* does not remove all six degrees of freedom. Figure 2-5 shows a roller/slider being applied to a face within SolidWorks. The green arrows represent the direction that is being held to zero displacement, meaning that in this example the beam could move horizontally in both directions (i.e., left/right and in/out of the page), but would not be able to move vertically. The direction of the arrows also represent the positive direction for a displacement boundary condition.

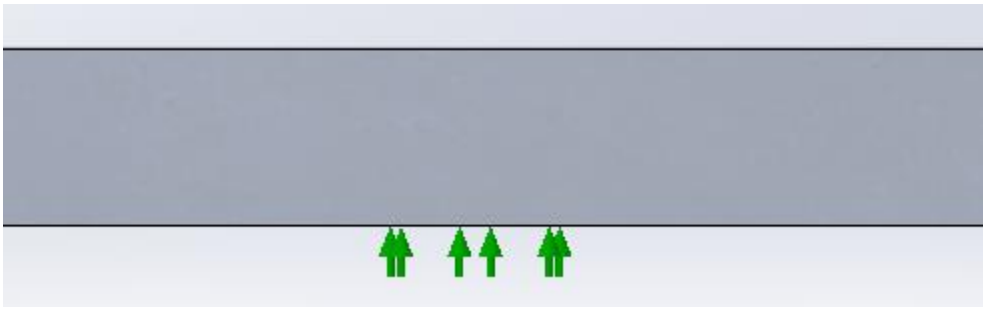

Figure 2-5: An example of a *roller/slider* fixture being applied to a face within SolidWorks simulation. The green arrows represent the positive direction along with the direction that is being held to zero displacement.

Displacement boundary conditions allow for more customization while creating a model, as they allow specific deformations to be applied. Figure 2-6 illustrates the use of a displacement boundary condition and shows the stress profile along the beam. A *fixed* fixture is used to restrain the left side while the right is being restrained with a roller/slider. A positive initial displacement was added to give the beam an initial curve. As can be seen, the beam deforms the desired distance and initial stresses have been calculated along the beam.

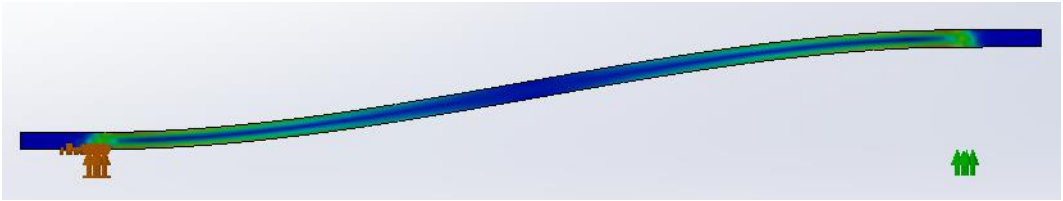

Figure 2-6: An example of the implementation of a displacement boundary condition. The left side was restrained using a fixed fixture while the right was held with a roller slider, which results in an initial displacement and stress profile.

2.4.3 Fixed Hinge and Bearing

Fixed hinge fixtures restrict cylindrical shafts from translating while allowing for the rotation around the axis of the shaft. In Figure 2-7, if the blue face is selected to be a *fixed hinge*, the component will be able to rotate around the axis of the shaft, but other translations and rotations will be restricted. While using this fixture, there is no friction on the selected surface, and lateral/axial stiffness cannot be modified.

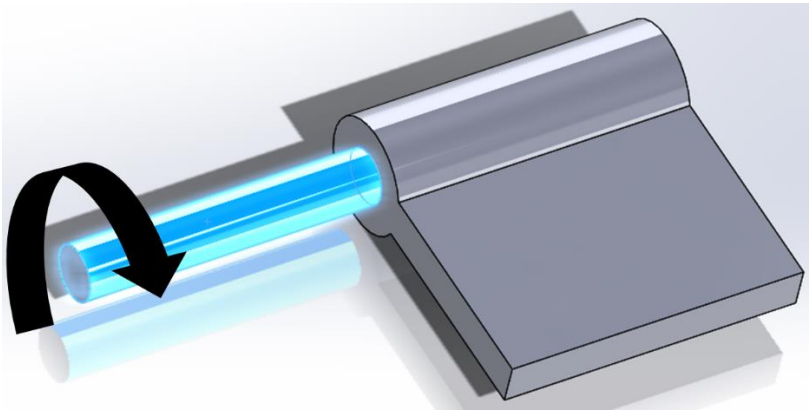

Figure 2-7: Illustration of how a *fixed hinge* restraint functions within SolidWorks.

However, this same cylinder could also be restrained with a *bearing* fixture. When using the *bearing* fixture Solidworks suggest that the cylindrical face length should have a length less than twice the diameter of the shaft. *Bearing* fixtures allow the same rotation as the fixed-hinged but also allow for the selection of a self-aligning bearing as well as axial and lateral stiffness. A setting to stabilize shaft rotation can also be selected, which applies a low torsional spring to the shaft face preventing the shaft from rotating freely. A freely rotating

face can lead to instabilities within FEA. Bearings are also connectors and will be discussed further in section 2.5.3.

2.5 Connectors

Connectors are features within SolidWorks that replace real hardware with virtual components, speeding up the simulation process and typically improving accuracy. Connectors allow for the rapid modification of several different conditions. These changeable conditions allow for a more accurate representation of how these connecting components interact with the rest of the assembly. An example of a connector condition is pre-tension within a bolt.

Faster simulation times are often achieved while using connectors because special element types are used for connectors: beam, rigid, and spring. Beam elements are line representations of the model, which are meshed and solved. Rigid elements are beam elements, but they have infinite stiffness. Spring elements are special beam elements, but they have finite stiffness and the user specifies this value. By using these elements the solver does not solve the stresses within the connector itself. Instead, only interactions between the connector and the face the connector contacts are solved. If enough conditions are specified the solver also checks to ensure the connector is strong enough for the given application (Dassault Systemes, 2019). Connectors reduce the number of contact sets within the model, which can significantly decrease simulation times. The implementation and modifiable conditions of *pin, bolt, and bearing* connectors will be discussed in the following sections.

2.5.1 Pin Connectors

Pin connectors within SolidWorks are beam elements that allow translation along the axis of the pin as well as rotation about the axis. However, pins can be simulated with retaining rings, fixing all translation. A pin with a key can also be simulated, fixing rotation. SolidWorks simulates fixed pins by designating high rotational and axial stiffness values to the two cylindrical faces that the pin contacts. Custom stiffness values can also be set to these two DOFs. This modifiable condition allows for the modeling of slip and press fits, although these

values must be known or experimentally determined. Other options allow the user to specify the material of the pin as well as the tensile strength and connection limitations.

In SolidWorks, any two concentric cylinders can be connected with a pin. Pins can be used on cylindrical faces with different diameters and can be used on faces that are not coincident. This means that pins can also be used to replace large rods. To insert pins into the model, the two cylindrical faces with which the pin is in contact are selected, along with the desired conditions.

2.5.2 Bolt Connectors

Bolt connecters join two or more components, not allowing the attached component to rotate or translate with respect to the rest of the assembly. SolidWorks models the shank as a tension-only beam element and the head and nut are modelled as rigid bar elements (Dassault Systems, 2019). The shank is a tension-only beam element as this allows preloading to be modeled. Bar elements are used to connect the shank to a hole if they have matching diameters. This allows shear effects to be modeled. Due to the rigid bars used on the faces of the bolt head and nut, the stresses in these regions may not be accurate. However, at about one bolt diameter from the bolt connector these inaccuracies become negligible (Dassault Systems, 2019).

While using bolts in SolidWorks the users can select the bolt type, shank diameter, head diameter, material, bolt strength data, preload conditions, and friction factor. The five available bolt types are counterbore with nut, countersink with nut, counterbore screw, counter sink screw, and foundation bolt. After solving a simulation with bolt connectors, the simulation provides the forces on the bolt and shows whether the bolt can withstand the forces being applied to it. This allows for a quick check on these connections. By using the virtual bolts, the stress distribution on the bolt itself is not calculated. To see the stress profile on a bolt, the bolt must be modeled and implemented using contact sets, defining the interactions between component and bolt.

2.5.3 Bearing Connectors

Virtual bearing connectors are used to connect two cylindrical surfaces by acting like a ball or roller bearing. The surfaces are typically the shaft and the housing that the bearing contacts. Bearing connectors differ from the bearing fixtures, as they connect a shaft to a housing while the bearing fixture connects a shaft to a virtual ground. Since the fixture connects to virtual ground, the component is connected through the bearing to a virtual housing with infinite stiffness. When using these connectors the housing is able to deflect.

SolidWorks can simulate both self-aligning or non-self-aligning bearings. Self-aligning bearings allow for off-axis rotation while non-self-aligning bearings restrict this movement. By restricting this movement, moments develop on the housing face that the bearing contacts. Non-self-aligning bearings typically replace roller or needle bearings, while self-aligning bearings correspond to bearings with two rows of balls with a common concave sphered raceway in the outer ring.

The axial and lateral stiffness of *bearing* connectors can be defined by making the bearing rigid or flexible. When a rigid bearing is selected, very high stiffness values are used which do not allow the selected faces to translate or deform. Flexible bearings allow for limited local flexibility and for the user to change the stiffness values. However, bearing connectors are modeled linearly in SolidWorks. Figure 2-8 illustrates the expected behavior of an actual bearing (red line), and how bearing connectors are modeled (grey line). K1 and K2 represent the two stiffnesses expected when applying a load to a bearing and deforming it. By changing the axial and lateral stiffness values within SolidWorks the slope of the bearing connector changes.

As seen in Figure 2-8, it is important to define bearing stiffness values that result in an intersection at a force close to the bearing's real-world application since deviations from this force can lead to significant error. Other nonlinearities exist within bearings such as clearances and Hertzian contacts (i.e., contacts between two curved surfaces) between the balls and the race (Raabe, 2018). However, through experimental testing, reliable approximations of these stiffness values can be determined.

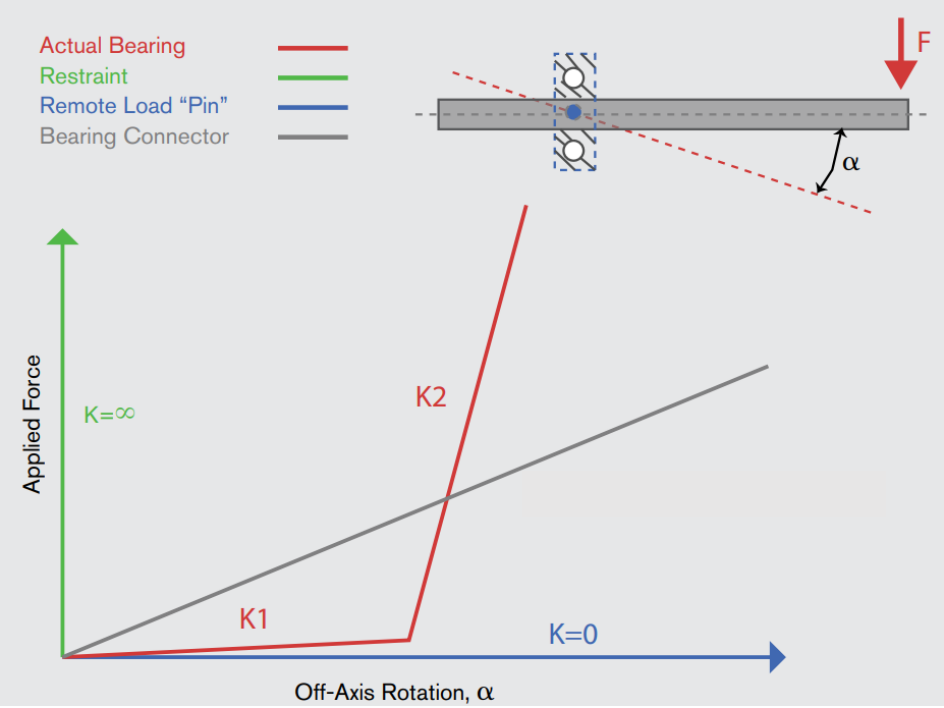

Figure 2-8: Illustration of how bearings are modeled within SolidWorks. The top right image illustrates the loading condition of the bearing. The red line represents an expected deformation from an actual bearing while the grey shows the bearing connector feature. (Dassault Systemes, 2019)

2.6 Contacts

Contact sets define the interactions between components under load in an FEA assembly. FEA components are meshed separately, meaning at locations where these components contact each other, the interactions must be defined. More specifically, the interaction between nodes of individual components on nearby nodes of other components must be defined. These nodes can be joined or left independent and can lead to different results. The interference detection tool, mentioned above, should be used before defining contact sets. This ensures that components are touching correctly, and the contact sets are being defined as expected.

When defining contact sets, there are three levels: global, component, and local. The top level sets are global contact conditions, which define all areas that share two faces

throughout the entire assembly. Component contacts define the interactions between areas shared by selected components. These contact conditions override any global contact sets. Local contact sets define the interactions between entities such as faces, edges, and vertices between components. These contact sets override both component and global conditions (King, 2018).

There are five ways to define the interaction between nodes of component meshes: *bonded, no-penetration, allow-penetration, shrink fit,* and *virtual wall*. Each of these change how the touching entities interact with each other and should be chosen with care. However, *no-penetration* contact sets require more computational power and significantly increase simulation times.

Bonded contact sets adhere the touching entities together by creating compatible meshes and then joining the shared nodes of these entities. By joining these nodes, continuity is ensured and the load is transferred between the two entities. An example of the *bonded* contact set can be seen in Figure 2-9. In this image, the touching faces are bonded, transferring the load between the beams and staying in contact along the entire bonded face.

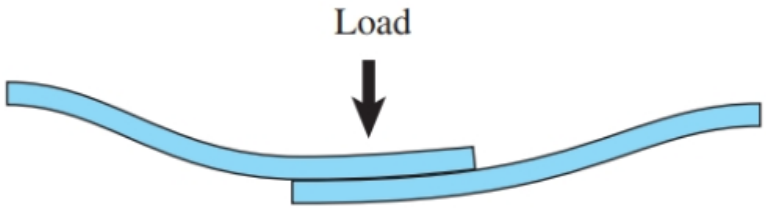

Figure 2-9: Bonded contact set. Image from (King, 2018).

No-penetration contact sets do not allow the components to interfere or penetrate, but also allow for gaps under certain loading conditions. An example of the no-penetration contact with a collision and gap can be seen in Figure 2-10. While using the no-penetration contact, the meshes are still compatible; however, the nodes are not joined. When gaps exist, gap elements are created to connect the coincident nodes filling the empty space. This contact relies on friction coefficients that are specified within the material properties of the study.

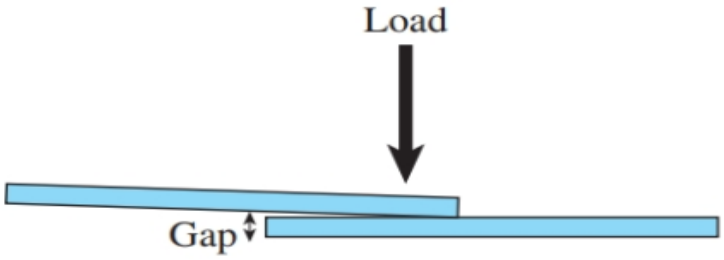

Figure 2-10: No-penetration contact with load causing gap. Image from (King, 2018)

The *allow-penetration* contact treats the components as two disjointed entities, allowing them to penetrate/interfere as well as not transferring any forces. This contact set also allows for gaps to form; both cases can be seen in Figure 2-11.

Virtual-wall and *shrink fits* are niche contact sets and allow for more customization within the model. The *virtual-wall* defines a rigid or flexible plane that the components will interact with under conditions that cause contact. The friction coefficient between the wall and entities can be modified to represent any desired surface. The *shrink-fit* contact is used on entities that have interferences prior to the study, such as press fits.

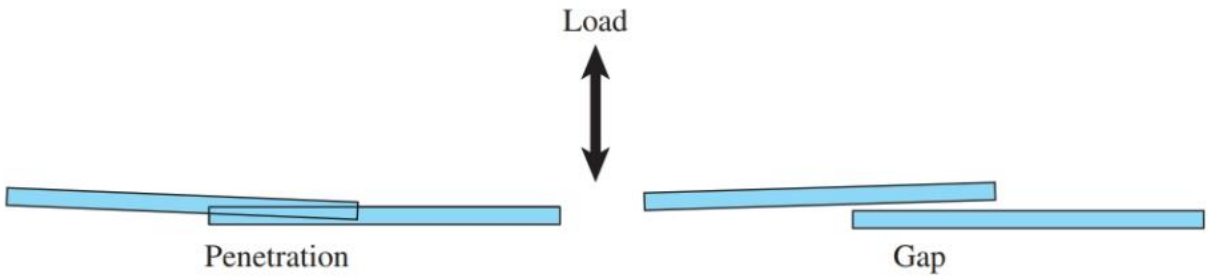

Figure 2-11: Allow-penetration contact being used under two loading conditions. Image from (King, 2018)

2.7 Forces

When simulating a force in FEA with an approximate representation, it should be applied in a way that mimics physical reality as closely as possible. Forces within SolidWorks can be applied to faces, edges, vertices, or reference points. When applying a force or load to a component, three parameters must be defined: the entity that the load will act upon, a reference entity for the direction of the force, and the direction of the force

relative to the reference entity (King, 2018). When choosing these parameters, if a reference is chosen on a location of the component that deflects, the force will follow the reference throughout the study. If this is not desired, planes or rigid components can be selected to ensure the force's orientation does not change.

Forces are only applied to the nodes during a simulation, and if edges, points, or lines are selected to apply forces, high, inaccurate stress results can be generated. To avoid this, forces should be applied as total forces, or pressures, as this lowers the local stresses. Saint-Venant's principle states that "*If the forces acting on a small portion of the surface of an elastic body are replaced by another statically equivalent system of forces acting on the same portion of the surface, this redistribution of loading produces substantial changes in the stresses locally, but has a negligible effect on the stresses at distances which are large in comparison with the linear dimensions of the surface on which the forces are changed.*" (Sonnerlind, 2018). Essentially, this principle states that by turning a force into a statistically equivalent pressure it will lower the local stresses, but will not compromise the study. An example of this principle can be seen in Figure 2-12. In all three cases, the stresses at the critical point are the same, but the point load displays extreme local stresses at the location of the force in comparison to the other two tests.

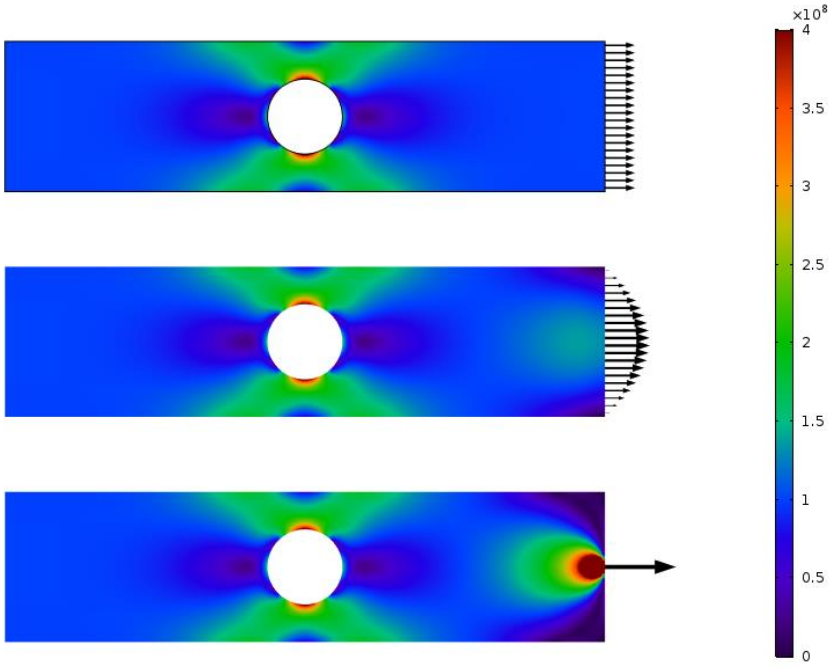

Figure 2-12: Example of Saint Venant's principle. As can be seen, the three different statistically equivalent forces have the same result at the critical point. It can also be seen the point loads local stress is far higher than any other. Image from (Sonnerlind, 2018).

Due to the flexibility of FEA, poor assumption can lead to inaccurate results and incorrect design decisions. To verify the FEA practices used on the BLUE SABINO components, experiments were performed to compare the deflection of a manufactured assembly to the results predicted by a SolidWorks FEA. The following chapter describes the methods of this experiment as well as the configuration of the FEA.

3 METHODS

3.1 Overview

As stated previously, FEA can be an incredibly useful tool but accurate results can be difficult to obtain. Assembly 1005 from the BLUE SABINO, seen in Figure 3-1, is the mechanism that allows the user to perform internal/external rotation (i.e., rotation of the upper arm about its long axis) while using the exoskeleton. This four-bar mechanism allows the arm cuff to revolve around a remote center without encompassing the patients arm. This makes the donning and doffing process easier for stroke patients and therapists, but consists of several bearing and bolt connections that are difficult to model within an FEA. Due to this difficulty, three experiments were performed to compare how well the deflection of the actual assembly related to the FEA deflection results.

The experimental setups are composed of an Instron 5944 single column universal testing system (UTS) that performed a compression test while recording the force applied and the deflection. During two of the experiments, a loading nose attached to a 2kN load cell descended at a rate of 0.03mm/s up to a 200N load. At 200N, the loading nose rose at a rate of 0.03mm/s until the load was relieved. During the other experiment the load went up to 300N, using the same rates. These values were chosen because they are the expected loads on these components.

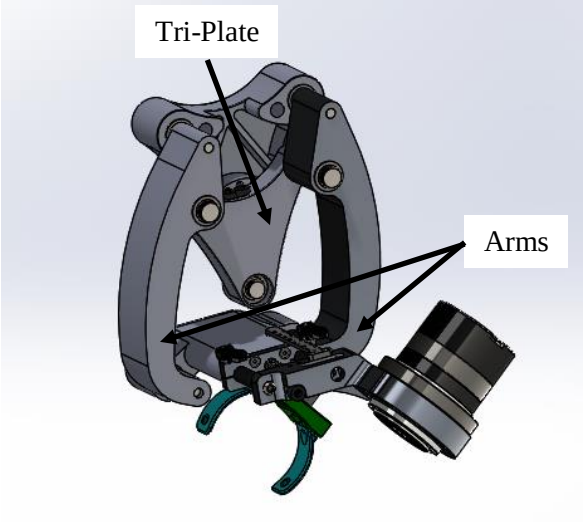

Figure 3-1: Assembly 1005 of the Blue Sabino project

3.2 Control Test

A control test was designed in order to compare results without bearings in the model. The tri-plate, of assembly 1005, was bolted to two 6063-T4 aluminum plates and placed on a larger block of 6063-T4 aluminum to elevate the component into the UTS's working range, as seen in Figure 3-2. The UTS's column restricted the components from moving backwards, and due to the direction of the applied force no other restraints were required. Two 1.75mm shim-like features extrude from the Tri-Plate to the base plates at the bolting location, with only one being visible in Figure 3-2. This extrusion eliminated all other contacts that could occur between the Tri-Plate and the plates during the experiment. The 200 N load was applied vertically on the outer ring of the bearing mount with a loading nose. This experiment was repeated seven times to ensure no sliding occurred during testing.

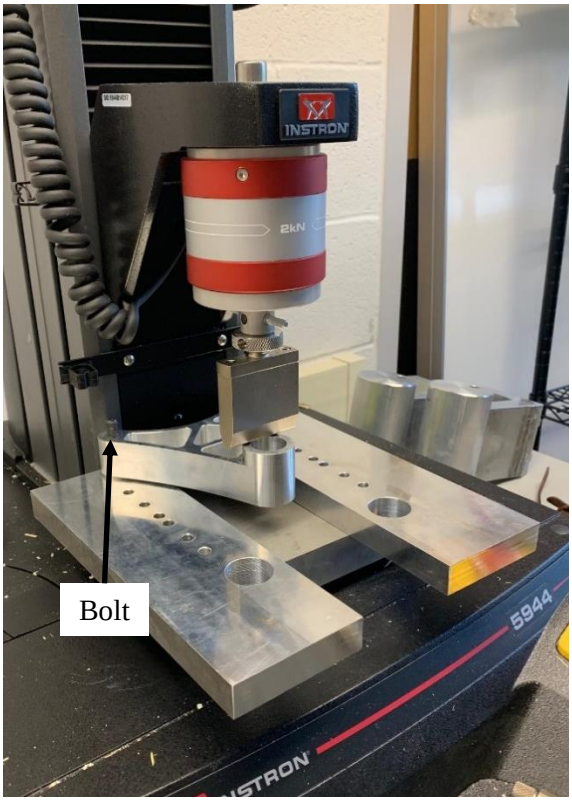

Figure 3-2: Control test to verify FEA without bearings.

3.3 Bearing Tests

Two separate experiments were performed to verify the FEA model with bearings. These two experiments can be seen in Figure 3-3. The assembly was bolted to the two aluminum plates at the distal ends of the Arms along with flanged bearings fitting into two close-fit holes. To lock the assembly in place, bolts fastened the two aluminum base plates to the UTS. The left image shows the lower test with the force applied in the center of the hole, and the right image shows the upper test, with the force applied on the outer edge of the ring. For the rest of this paper, the left image will be referred to as the *lower bearing* test and the right image will be the *upper bearing* test. A compression test was selected because the applied forces were similar to the real-world application of this assembly.

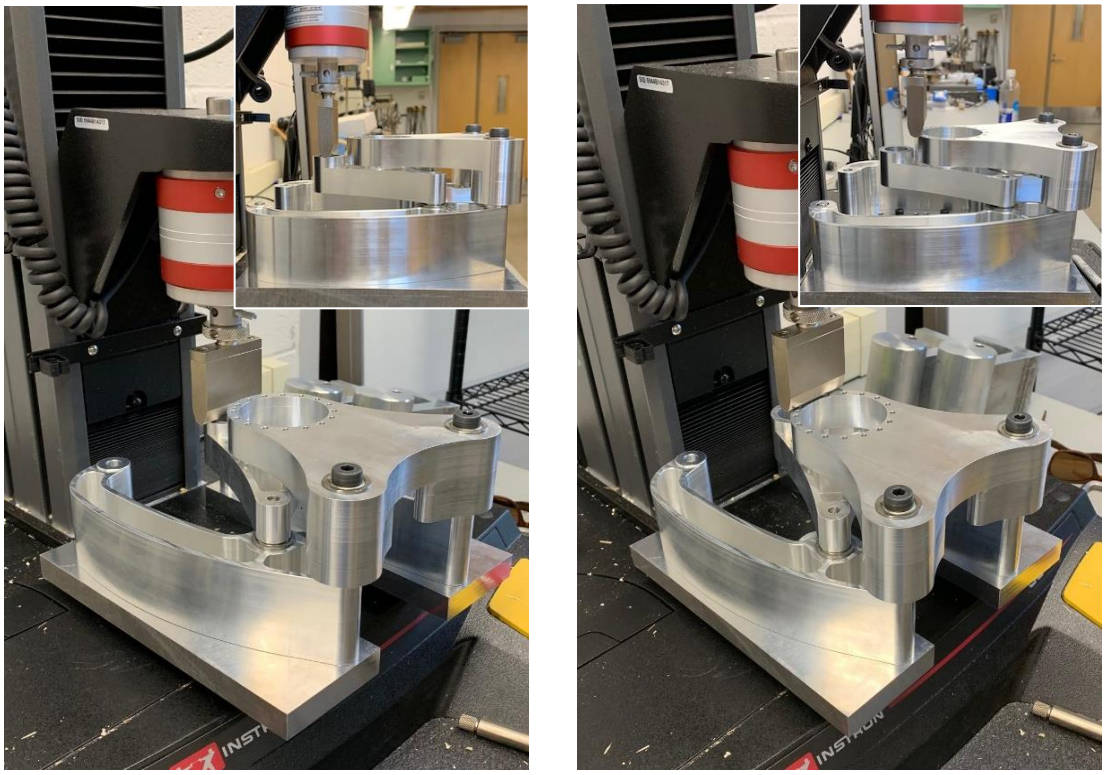

Figure 3-3: Experimental bearing test setups with the left being the *lower bearing* test and the right being the *upper bearing* test. Inset images in the upper right of each image further illustrate the different loading conditions of the two tests.

3.4 FEA: Control Test

During the *control test*, base plates, bolts, and the component were modeled and assembled to mimic the experimental setup, as seen in Figure 3-4. *Fixed* fixtures restrained the "Base Block" and a 200N force was applied along a 2mm strip on the bearing ring of the component. Mock bolts, with diameters matching the diameter of the component's holes, connected the component to the "Base Plates". The bolt heads pressed against the underside of the base blocks while the last 4mm of the threads were *locally bonded* to the component. A *bonded* connection joined a 1mm strip of the Base Plates to the Base Block, denoted by "Bonded" in Figure 3-4. This allows the Base Plates to bend along their length while also restraining the model from sliding. A global *no penetration* contact set defined all other coincident faces. Multiple simulations with different curvature-based meshes were processed

to compare time efficiency to accuracy. This comparison influenced the mesh decision of the *upper* and *lower bearing test.*

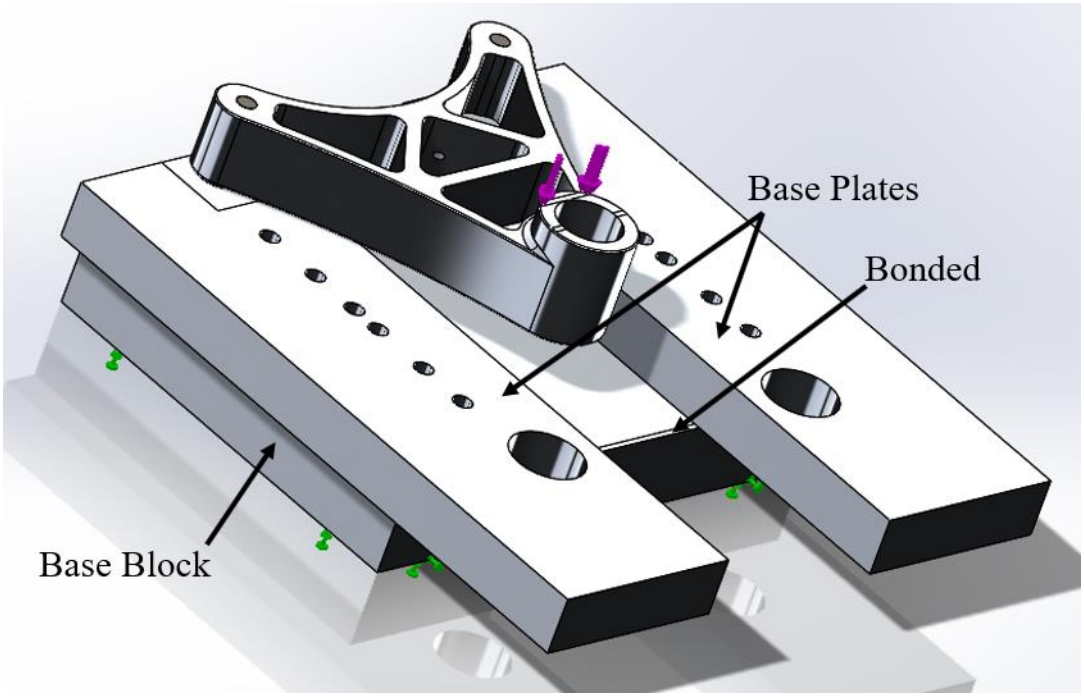

Figure 3-4: Control Test FEA setup. Fixed fixtures restrained the base block (green arrows) while a force was applied on the bearing ring (purple arrows). "Bonded" designates the location of a 1mm strip used to bond the base plate together.

3.5 FEA: Upper and Lower Bearing Test

During this set of simulations, both tests had identical settings with the only difference being the location of the applied force. The components were assembled to mimic that of the experiment and split-lines were used to create selectable surfaces for *bearing connectors* and *bonded* faces. A *fixed* fixture on the bottom of both base plates restrained the assembly, denoted by the green arrows in Figure 3-5. Mock shoulder bolts joined the components with matching thread and hole diameters, resulting in touching faces along the bolt after the *bearing* connections. A *bonded* contact set joined the last 4mm of each bolt to its corresponding component. *Bonded* contact sets also connected the assembly to the base plate, denoted by the blue highlighted areas in Figure 3-5. A global *no penetration* contact set defined all other coincident faces. Eight flexible, self-aligning *bearing* connectors joined the components to

corresponding bolts. These connectors were 6mm wide to represent the bearings used in the experiment. A curvature-based mesh with a maximum element size of 0.3243in, minimum element size of 0.0649in, minimum number of elements in a circle of 8, and element size growth ratio of 1.4 was used, along with a mesh control (element size 4.01; element ratio 1.5) on the base plates to reduce computational cost. This resulted in a mesh with 159,460 elements and 265280 nodes. Using meshes with lower element counts showed similar results, but had larger errors. This indicated that there were no oddities due to the mesh.

Simulations with a variety of different axial and lateral stiffness values were evaluated to find values that resulted in accurate deformations, compared to experimental results, for both the *upper* and *lower bearing test* simultaneously. A cost function, given as:

$$C = |U| + |L| + |D|$$

with U being the error percentage of the *upper bearing test*, L being the error percentage of the *lower bearing test*, and D being the difference of the errors was used to compare the results to find the best set of stiffness values. Optimal stiffness values, determined by the cost function, were used to compare the error of the simulation over a range of 250N for the *upper bearing* test and 150N for the *lower bearing* test to further understand the inaccuracies over these working ranges.

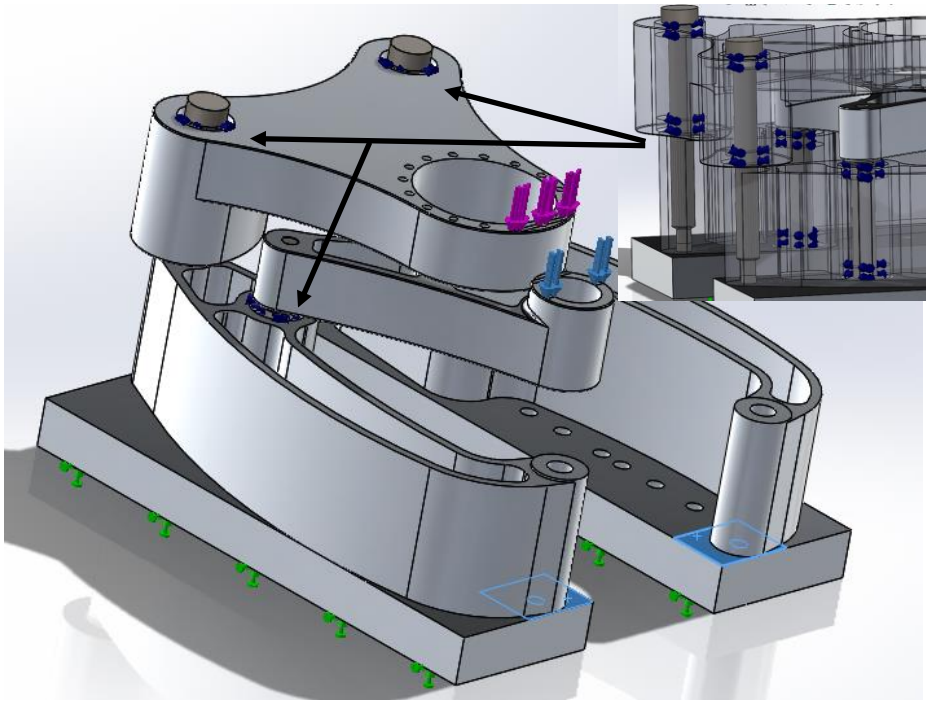

Figure 3-5: FEA setup for *upper* and *lower* bearing test. The purple and light blue arrows represent the force locations for the *upper* and *lower bearing* test respectively. The green arrows represent the fixed fixture used to restrain the base plates. The dark blue arrows, seen in the inset view in the top right, represent the bearing connectors with three bearing locations being designated by the black arrows. The highlighted blue faces show the location of the *bonded* contact sets.

4 RESULTS

4.1 Control Test

The results of the experimental control test can be seen in Figure 4-1. During all seven tests, the loading nose contacted the assembly at 0mm deflection and continued loading until reaching the 200N threshold, upon which the nose would retract. This process resulted in each loading and unloading having hysteresis as well as slightly more deflection from test to test. However, the range of maximum values is 0.0055mm, with an average of 0.253mm of deflection. This average displacement at 200N (0.253mm) was used to compare the experimental setup to the FEA simulation.

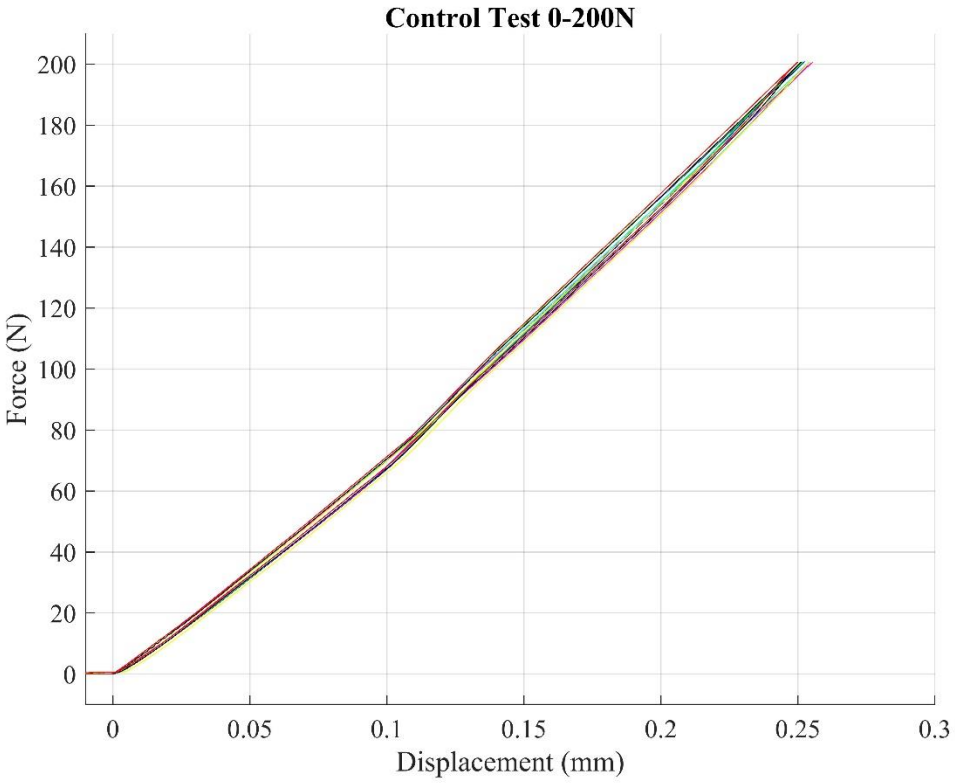

Figure 4-1: Results of the seven experimental control tests. The force contacts the assembly at 0mm in all seven trials, resulting in a range of 0.2499mm to 0.2554mm at the maximum dispalcement.

To find a mesh that provided accurate results and reasonable simulation times, a variety of different meshes were tested at 200N, resulting in Figure 4-2. Error corresponds to the error of the simulation compared to the experimental data, with positive error signifying that the simulation was stiffer than the experimental. The faster, coarser meshes resulted in higher errors, while the finer meshes took significantly more time, but reduced error. The red "x" indicates the selected mesh, described in section 3.4 that was used during the bearing simulations. This mesh in the control test had an error of 6.6%.

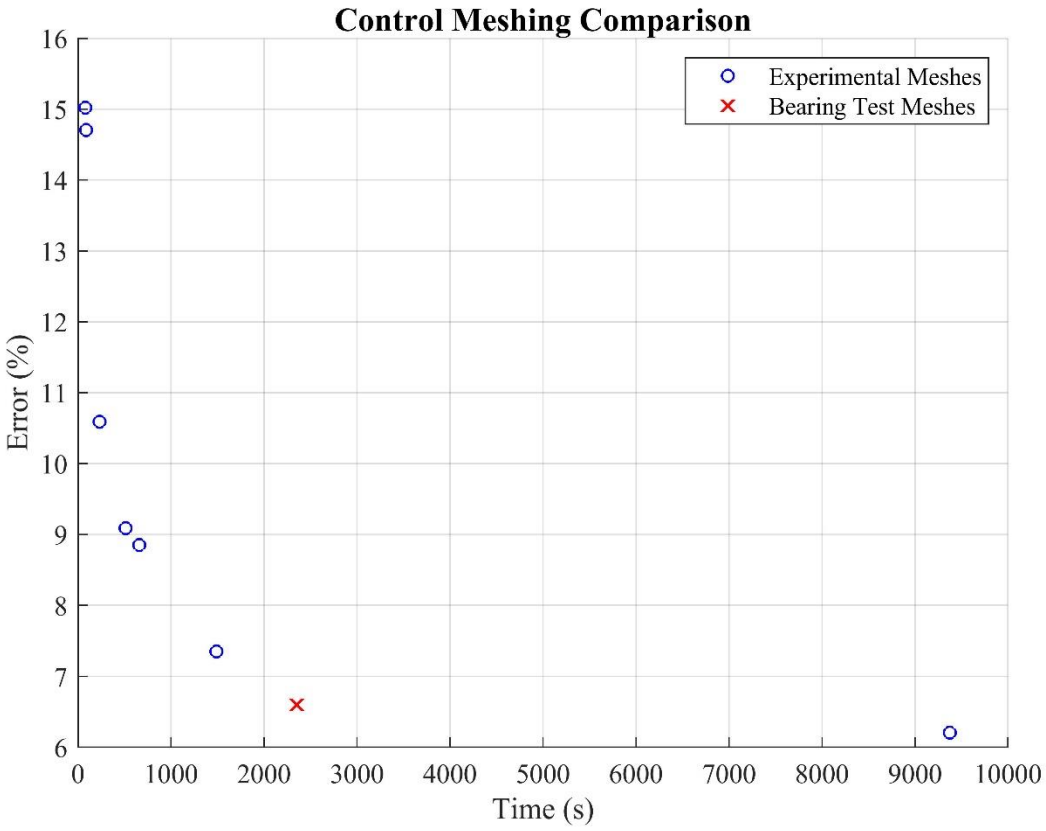

Figure 4-2: Results for control test with varying meshes. Error corresponds to the deflection error of the simulation compared to the experimental data at 200N. Points that required more time had finer meshes (more elements) with the red "x" indicating the mesh used for the *bearing* tests. Positive error corresponds to the model being too stiff, i.e. the simulation deflected less than the experimental setup.

4.2 FEA: Determining Bearing Stiffness

To find optimal axial and lateral stiffness values, 23 sets of data points were used to create a point cloud, as seen in Figure 4-3. In this graph, positive error values indicate that the simulation was stiffer than the experiment, similar to the control test. As stiffness values approach 3.5e7 N/m (lateral) and 3.75e5 N/m (axial), the errors of both *upper* and *lower bearing* tests approach zero, ultimately reducing the error between the two tests at 200N. These stiffness values resulted in errors of -1.04% and -0.28% for the *upper* and *lower* bearing tests respectively.

Data points not displayed in Figure 4-3, such as stiffness values with high lateral stiffness and low axial stiffness, were excluded from the results. These locations resulted in either collisions within the simulation or extremely high errors.

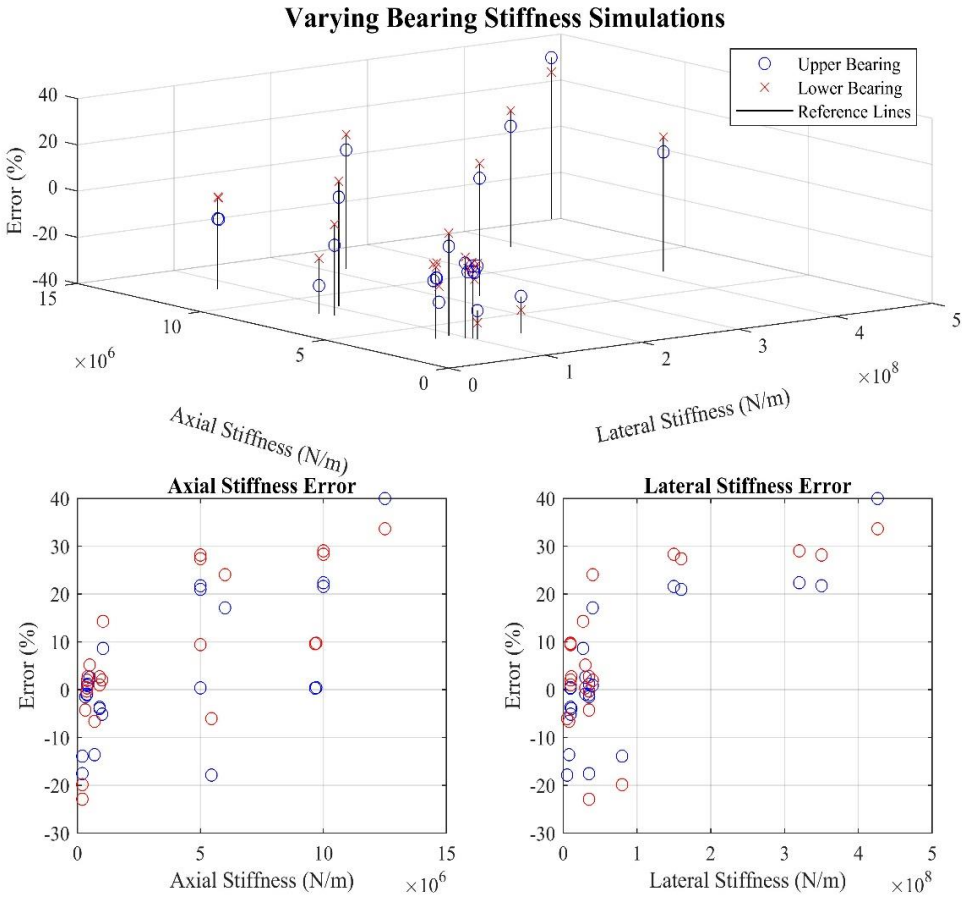

Figure 4-3: Raw simulation data generated by varying the axial and lateral stiffness values in the bearing test. The lowest errors for both simulations, compared to their experimental counterparts, are located around a lateral stiffness of 3.5e7 N/m and an axial stiffness of 3.75e5 N/m. The bottom two graphs allow for easier visualization of the lateral and axial effects on the model.

The results of processing this data through the cost function can be seen in Figure 4-4. These images are top down views of Figure 4-3 with a color map describing the total cost error of each set of data. In the left image a blue cluster can be seen in the lower left corner, indicating a location where both the *upper* and *lower bearing* tests are close to zero error. The right image focuses in at this location and illustrates that a lateral stiffeness of 3.5e7 N/m and an axial stiffness of 3.75e5 N/m provide the lowest cost, with a value of 2.09.

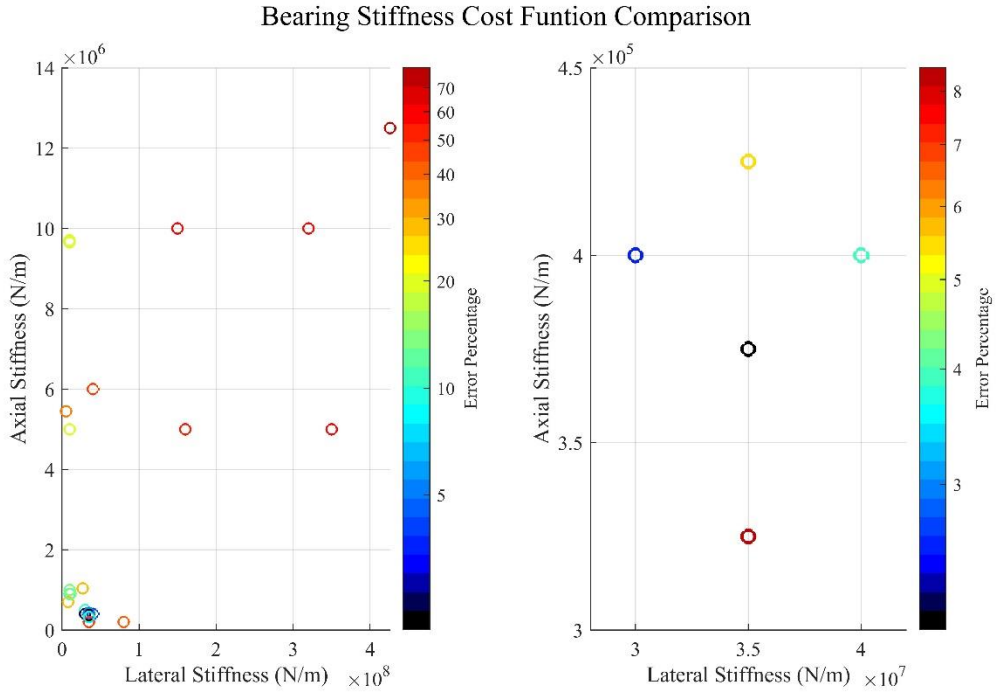

Figure 4-4: Graphical representation of how changing the axial and lateral stiffness affects the cost function. The left image represents all 23 sets of data points while the right focuses in at the critical location with the lowest overall error.

4.3 FEA: Variable Force Bearing Test

The *upper* and *lower bearing* tests showed different bearing characteristics during the experimental tests, seen in Figure 4-5. The experimental *upper bearing* tests showed three distinct slopes as the load intensified, while the *lower bearing* tests had a consistent slope throughout the loading phase. However, both simulation solutions were linear. Using a linear regression, the *upper* and *lower bearing assemblies* having a standard error of 0.083N and 0.012N respectively. The range at 300N was 0.0038mm for the *upper bearing* test and 0.001mm for the *lower bearing* test at 200N, indicating a rigid connection to the UTS. At 200N the error of the *upper bearing* and *lower bearing* test were -1.04% and .282% respectively. The *upper bearing* test resulted in a maximum error of 24.65% while the *lower bearing* test's maximum error was 3%, both occurring at 50N.

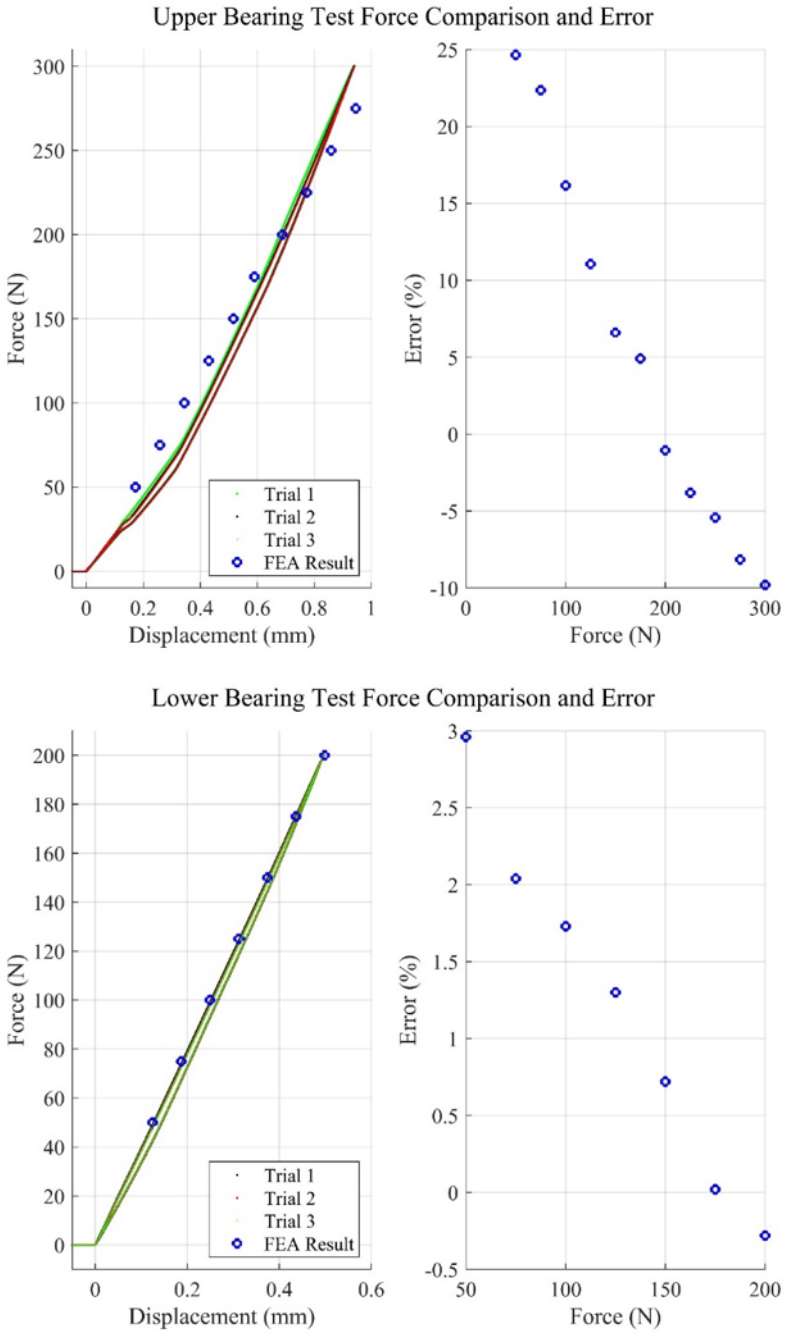

Figure 4-5: Comparison of the experimental and simulation results over a range of 250N for the *upper* bearing test and 150N for the *lower* bearing test. Results suggest a better fit for the *lower* bearing test as the experimental data was more linear than the *upper* bearing test.

4.4 Control Test Discussion

Due to the assembly not being fixed to the UTS there was slight movement during the experiment. This is apparent as the range at 200N was larger in this test than for both bearing tests. However, the movement was small enough that fully fixing the assembly was been unnecessary. Multiple attempts to place the assembly in the UTS as well as the reconstruction of the assembly were not performed. However, careful assembly placement and evenly torqued bolts during the assembly process should result in similar results because it closely matches the simulation.

The bearing tests required many simulations, meaning a mesh that had a reasonable simulation time that did not overly degrade accuracy was required. Figure 4-2 shows that the tradeoff between accuracy and simulation time varies with an exponential decay. From the graph, the red “x” is close to the asymptote and any further refinement of the mesh will result in slight accuracy improvements while causing significantly longer simulation times, making it the most suitable mesh.

4.5 Bearing Tests Discussion

From the data seen in Figure 4-5, it is apparent that the two bearing experiments had different characteristics. When modeling bearings, two distinct slopes are typically expected, as seen in Figure 2-8. It is believed that the multiple slopes displayed in the *upper bearing* test are attributed to the multiple bearings within the assembly. Not all bearing are manufactured identically and the press fits within the assembly are all slightly different. This results in some bearing being having the balls fully engaged, while others still have clearances between the ball and outer race. With force gradually ramping up, the bearings with clearances will eventually engage, resulting in a stiffer assembly. This causes multiple slopes, with the final steep incline being when all bearings have fully engaged. The experimental *lower bearing* test did not exhibit the same behavior. This is believed to be the result of tighter press-fits, causing the bearings to have a greater pre-load than the *upper bearing* test. With tighter press-fits the bearings are believed to have passed the threshold of the first expected slope, resulting in one

uniform slope throughout the experiment. Due to the nature of these interactions, each manufactured assembly will have slightly different deflection characteristics.

Both simulations become increasingly inaccurate when forces move away from 200N, with the *upper bearing* test being more exaggerated. The increased error within the *upper bearing* test was expected due to the three distinct slopes. With press fits that caused the experimental *upper bearing* test to resemble that of the *lower bearing* test, lower errors are expected. However, the force exerted on this assembly in its normal application is roughly 200N. This means that for design purposes this simulation can accurately predict the deflection of the entire assembly.

5 CONCLUDING REMARKS

5.1 Previous FEA Methods

As mentioned previously, other FEA methods were attempted prior to the methods discussed in this thesis. These methods included mock bearing of various material and using different contact sets on the bolts, both resulting in poor results. The mock bearings used during simulations were steel, brass, and ABS plastic. The bearings were modeled to mimic the shape of the bearings, but were solid bodies. The mock bearings were *bonded* to the bolt's shaft and the component's housing for the bearing. The simulations took minimal time, but resulted in significant error. For the *upper bearing* test the error for the brass, steel, and ABS were 82.8%, 82.1%, and 61.1% respectively, and 75.8%, 77.3%, and 47.6% respectively for the *lower bearing* test. Upon realizing these errors, it was apparent that solid bodies were not appropriate for estimating the bearing deflections within the BLUE SABINO linkages. It also showed that the main cause of deflection in the assembly is from the bearings themselves. To significantly minimize deflection, stiffer bearings or geometrical changes are required.

While modeling the simulations as described for the control test, an error was present showing that the simulation was stiffer than the experiment. The main cause for this was believed to be the amount of thread that was being bonded to the components. Simulations were performed with all the threads, the last 4mm of thread, and the first 4mm of thread being bonded. For this simulation the errors were 38.22%, 9.68%, and 29.36% respectively. Since the last 4mm of thread being bonded produced the most accurate results, this was used for all of the tests. It is believed that this assumption was acceptable because when bonding a steel shaft to the aluminum component it provides a much stronger connection than what is present in the physical model. It is also common for threads to be modeled with only a few threads as they will support the majority of the load.

5.2 Future Work

With the model described in this thesis, a better estimate than previously possible can be achieved for the 1005 assembly, as well as other assemblies with similar bearing

connections within the BLUE SABINO project. The main concern when designing these components is cumulative deflection at the fingertips. To move forward, a comprehensive simulation of the entire 1005 assembly should be performed to estimate the amount of deflection that is expected at the fingertips. The resulting deflection can then be used to determine if the assembly is stiff enough. If it is not, design changes can be made to improve the overall stiffness. In the model with *bonded* solid steel bearings, it can be assumed that the deflection represents an assembly without bearing deflection. Comparing this model to the model described in section 3.4 an approximate deflection, caused by the bearings, was found to be 0.570mm for the *upper bearing* configuration and 0.378mm for the *lower bearing* configuration. This result shows that a redesign of this assembly should focus on the selection of stiffer bearings rather than the design of more rigid components.

A similar test could also be performed on other similar linkages within the project. Similar steps would be taken, but only the bearing test would be required since the same mesh and configurations should still be applicable. Different forces would be applied to the components as well as different bearing stiffnesses, but even without changing the stiffness values, a better estimate than previously obtained is possible.

5.3 Closing Remarks

Overall, the simulations provided accurate displacements for the assembly, at its anticipated load, while showing that the bearings are the greatest cause of deflection. Future redesigns may see the implementation of different bearings within the assembly, further minimizing the overall deflection. By using the same methods described above, reliable estimates for future assemblies' deformations can be obtained to find more optimal designs. The design should reduce deflections while maintaining or decreasing the current mass, ultimately leading to a more rigid and lightweight exoskeleton.

References

Adamson J., Beswick A., Ebrahim S., “Is Stroke the Most Common Cause of Disability?” *Journal of Stroke and Cerebrovascular Diseases*, vol. 13, no. 4, July 2004, pp. 171–77. *ScienceDirect*, doi:10.1016/j.jstrokecerebrovasdis.2004.06.003.

Akin, J. E. *Finite Element Analysis Concepts: Via SolidWorks*. World Scientific, 2010.

Benjamin, E. J., et al. “Heart Disease and Stroke Statistics-2017 Update: A Report From the American Heart Association.” *Circulation*, vol. 135, no. 10, Mar. 2017, pp. e146–603. *europepmc.org*, doi:10.1161/CIR.0000000000000485.

Bourdon, A., J. F. Rigal, and D. Play. "Static rolling bearing models in a CAD environment for the study of complex mechanisms: Part II—complete assembly model." (1999): 215-223.

Brändlein, Johannes. *Ball and Roller Bearings: Theory, Design, and Application.* John Wiley, 1999.

Bureau, US Census. “Older People Projected to Outnumber Children.” *The United States Census Bureau*, https://www.census.gov/newsroom/press-releases/2018/cb18-41-population-projections.html. Accessed 10 July 2019.

Dassault Systemes, Goengineer.com. (2019). [online] Available at: http://www.goengineer.com/wp-content/uploads/2014/04/Understanding-Connectors.pdf [Accessed 5 Nov. 2019].

Gargiulo, E. P. "A simple way to estimate bearing stiffness." Machine Design 52.17 (1980): 107-110.

Guo, Yi, and Robert G. Parker. "Stiffness matrix calculation of rolling element bearings using a finite element/contact mechanics model." *Mechanism and machine theory* 51 (2012): 32-45.

Harris, Tedric A. *Rolling bearing analysis.* John Wiley and sons, 1990.

Jones, A. B. "Analysis of Stresses and Deflections-New Departure Engineering Data." 1946.

Kelly-Hayes, Margaret “Influence of Age and Health Behaviors on Stroke Risk: Lessons from Longitudinal Studies.” *Journal of the American Geriatrics Society*, vol. 58, no. Suppl 2, Oct. 2010, pp. S325–28. *PubMed Central*, doi:10.1111/j.1532-5415.2010.02915.x.

Kelly-Hayes, Margaret, et al. “Time Course of Functional Recovery After Stroke: The Framingham Study.” *Journal of Neurologic Rehabilitation*, vol. 3, no. 2, June 1989, pp. 65–70. *SAGE Journals*, doi:10.1177/136140968900300202.

King, Robert H. *Finite Element Analysis with SOLIDWORKS Simulation*. Cengage Learning, 2018.

Lackland, Daniel T., et al. “Factors Influencing the Decline in Stroke Mortality: A Statement from the American Heart Association/American Stroke Association.” *Stroke*, vol. 45, no. 1, Jan. 2014, pp. 315–53. *PubMed*, doi:10.1161/01.str.0000437068.30550.cf.

Liew, Hoon-Voon, and Teik C. Lim. "Analysis of time-varying rolling element bearing characteristics." Journal of sound and vibration 3.283 (2005): 1163-1179.

Lim, Teik C., and Rajendra Singh. "Vibration transmission through rolling element bearings, part I: bearing stiffness formulation." *Journal of sound and vibration* 139.2 (1990): 179-199.

Logan, Daryl L. *A First Course in the Finite Element Method*. Cengage Learning, 2016.

Mozaffarian Dariush, et al. “Heart Disease and Stroke Statistics—2016 Update.” *Circulation*, vol. 133, no. 4, Jan. 2016, pp. e38–360. *ahajournals.org (Atypon)*, doi:10.1161/CIR.0000000000000350.

Page, Stephen J., et al. “Reconsidering the Motor Recovery Plateau in Stroke Rehabilitation1.” *Archives of Physical Medicine and Rehabilitation*, vol. 85, no. 8, Aug. 2004, pp. 1377–81. *www.archives-pmr.org*, doi:10.1016/j.apmr.2003.12.031.

Palmgren, Arvid. "Ball and roller bearing engineering." Philadelphia: SKF Industries Inc., 1959.

Perry, J. C., and J. Rosen. “Design of a 7 Degree-of-Freedom Upper-Limb Powered Exoskeleton.” *The First IEEE/RAS-EMBS International Conference on Biomedical Robotics and Biomechatronics, 2006. BioRob 2006.*, 2006, pp. 805–10. *IEEE Xplore*, doi:10.1109/BIOROB.2006.1639189.

Raabe, Markus. “You Need a Bearing Stiffness? Which One? | MESYS AG.” *MESYS*, 28 Sept. 2018, https://www.mesys.ag/?p=2313.

Schaechter, Judith D. “Motor Rehabilitation and Brain Plasticity after Hemiparetic Stroke.” *Progress in Neurobiology*, vol. 73, no. 1, May 2004, pp. 61–72. *ScienceDirect*, doi:10.1016/j.pneurobio.2004.04.001.

Shen, Y., et al. “Asymmetric Dual Arm Approach For Post Stroke Recovery Of Motor Functions Utilizing The EXO-UL8 Exoskeleton System: A Pilot Study.” *2018 40th Annual International Conference of the IEEE Engineering in Medicine and Biology Society (EMBC)*, 2018, pp. 1701–07. *IEEE Xplore*, doi:10.1109/EMBC.2018.8512665.

Simkins, M., et al. “Robotic Unilateral and Bilateral Upper-Limb Movement Training for Stroke Survivors Afflicted by Chronic Hemiparesis.” *2013 IEEE 13th International Conference on Rehabilitation Robotics (ICORR)*, 2013, pp. 1–6. *IEEE Xplore*, doi:10.1109/ICORR.2013.6650506.

Skilbeck, Clive E., et al. “Recovery after Stroke.” *Journal of Neurology, Neurosurgery, and Psychiatry*, vol. 46, no. 1, Jan. 1983, pp. 5–8.

Sonnerlind, Henrik. “Applying and Interpreting Saint-Venant’s Principle.” *COMSOL Multiphysics*, 22 Jan. 2018, https://www.comsol.com/blogs/applying-and-interpreting-saint-venants-principle/.